Supporting Information

The role of secondary organic matter on soot particle toxicity in reconstituted human bronchial epithelia exposed at the air-liquid interface

Zaira Leni[1‡], Michaela N. Ess[2‡], Alejandro Keller[3], James D. Allan[4], Heidi Hellén[5], Karri Saarnio[5], Katie R. Williams[6], Andrew S. Brown[6], Matthias Salathe[7], Nathalie Baumlin[7], Konstantina Vasilatou[2*] and Marianne Geiser[1*]

[1] University of Bern, 3012 Bern, Switzerland

[2] Federal Institute of Metrology METAS, 3003 Bern-Wabern, Switzerland

[3] University of Applied Sciences Northwestern Switzerland, 5210 Windisch, Switzerland

[4] University of Manchester, Manchester, M13 9PL, UK

[5] Finnish Meteorological Institute, 00101 Helsinki, Finland

[6] National Physical Laboratory, Teddington, TW11 0LW, UK

[7] Department of Internal Medicine, University of Kansas Medical Center, Kansas City, KS 66160 Kansas, USA.

[‡] Equal contributions

Supporting Information includes: 18 Pages; 3 Texts, 5 Tables, 7 Figures and 16 References

TABLE OF CONTENT:

Text S1. Optical properties of aerosols

An aethalometer AE33 [1], operated with a total aerosol flow of 2 L/min and an integration time of 1 s, was used to measure the change of light attenuation through a filter (370 - 950 nm). The built-in constants for the used filter tape were applied without any further corrections. The Ångström absorption exponent *AAE* was calculated from the absorption at all wavelengths. A Photoacoustic Extinctiometer (PAX) with wavelength of 870 nm was used to determine the eBC mass concentration and the single scattering albedo SSA of the generated soot particles at this wavelength. The PAX was calibrated according to a two-step process [2,3]: (i) with a polydisperse ammonium sulfate aerosol and (ii) with soot particles of high EC/TC mass fraction from the miniCAST 5201 BC generator. The sample flow was 1 L/min and the data averaging time was chosen to be 60 s, with background (zero) measurements of 1 min performed every 5 min. Mean value and standard deviation of the scattering coefficient b_{scat} and the absorption coefficient b_{abs} were calculated from at least 5 min of measurement. The single scattering albedo *SSA* at 870 nm was then calculated from the scattering and absorption coefficients. The eBC mass concentration was determined by using the *MAC* (mass absorption coefficient) value defined by the manufacturer (4.74 m^2/g at 870 nm).

Text S2. Off-line chemical analysis of aerosol particles

For OC/EC analysis, the aerosol was sampled on quartz fiber filters (Advantec, Japan, QR-100, 47 mm, prebaked at 500 °C for 1.5 h). For analysis with AMS, the particles were also sampled on quartz fiber filters (Advantec, Japan, QR-100, 47 mm, prebaked at 800 °C for 24 h). Sampling for analysis with GC-MS on PTFE membrane filters (Fluoropore 0.3 µm PTFE Membrane, Merck Millipore, Merck, Darmstadt, Germany). All filters were stored at −19 °C and shipped with dry ice to the different laboratories for analysis.

PAH (polycyclic aromatic hydrocarbons) were extracted from the filter samples using an automated Soxhlet extraction (Soxtherm Sox 416 Macro, C. Gerhardt GmbH & Co. KG, Germany) with dichloromethane. After extraction samples were dried with sodium sulfate, concentrated to 1 mL and cleaned using Florisil solid-phase extraction (SPE) cartridges. Afterwards the concentrations of PAHs were analyzed using a gas chromatograph-mass spectrometer (GC-MS, Agilent 6890N and 5973). For chromatographic separation, a J&W DB-5ms column (50 m, 0.25 mm i.d., film thickness 0.25 µm) and a 5-m pre-column (Agilent FS, USA) were used. Deuterated PAH compounds (phenantrene-d12, chrysene-d12, perylene-d12, and dibenzo[a,h]anthracene-d14, Dr. Ehrenstorfer) served as internal standards and were added to the extraction solvent before extraction. External standards (EPA 610 Polynuclear aromatic hydrocarbons Mix, Supelco, USA) with six different concentration levels were used. The [4,5] standards were followed. The analytical method has been described earlier, e.g. in [6].

Text S3. NACIVT deposition estimates

The deposited number of particles for the NACIVT experiments was calculated based on the deposition efficiency η reported earlier [7]. The discrete data given by the authors was approximated by

$$\eta(dp) = -0.098 \ln(dp) + 0.695, \quad \text{(Eq. S1)}$$

where dp is the mobility diameter in nanometers. For a given size distribution n(dp), the total deposited particle number per inset as a function of exposure time, t, is given by:

$$Ndep(t) = t\, Qins \int \eta(dp)\, n(dp)\, ddp, \quad \text{(Eq. S2)}$$

where Qins = 0.025 L/min is the individual inset flow rate. Finally, the deposited number of particles per cm^2 of cell culture area for the NACIVT can be obtained by dividing Ndep by the inset surface area s = 0.33 cm^2.

Similarly, the deposited aerosol mass per insert, M_{dep}, can be deduced from equation S2 using the effective density of the particles, ρ_{eff}, and the volume size distribution, $v(d_p)$, as

$$M_{dep}(t) = t\, \rho_{eff}\, Q_{ins} \int \eta(d_p)\, v(d_p)\, dd_p. \qquad \text{(Eq. S3)}$$

In our case, the effective density was calculated from $\rho_{eff} = M/V$, where M and V are the mass and volume concentration of the aerosol, measured by means of TEOM and SMPS, respectively.

Table S1. AAE and SSA_{870nm} of the different model aerosols generated in this study.

Series no.	Label	VOC	AAE (-)	SSA_{870nm} (-)
1	90 nm		1.27 ± 0.03	0.03 ± 0.01
1	90nm_coated_85nm	α-pinene	1.41 ± 0.01	0.13 ± 0.03
1	90nm_coated_100nm		1.53 ± 0.06	0.18 ± 0.01
1	90nm_coated_120nm		1.61 ± 0.06	0.28 ± 0.01
1, 5	90nm_coated_135nm		1.60 ± 0.03	0.37 ± 0.01
2	90nm		1.12 ± 0.02	0.03 ± 0.01
2	90nm_coated_85nm	mesitylene	1.23 ± 0.02	0.06 ± 0.01
2	90nm_coated_100nm		1.42 ± 0.02	0.16 ± 0.01
2	90nm_coated_120nm		1.60 ± 0.2	0.50 ± 0.01
3	30nm		1.37 ± 0.32	0.00 ± 0.01
3	30nm_coated_35nm	α-pinene	1.52 ± 0.01	0.00 ± 0.03
3	30nm_coated_45nm		1.57 ± 0.19	0.03 ± 0.01
3	30nm_coated_50nm		1.60 ± 0.19	0.08 ± 0.01
4	30nm		1.26 ± 0.15	0.00 ± 0.04
4	30nm_coated_35nm	mesitylene	1.57 ± 0.27	-
4	30nm_coated_45nm		1.70 ± 0.32	-
4	30nm_coated_50nm		1.50 ± 0.19	0.14 ± 0.16
5	90nm_coated_135nm_2	α-pinene	1.64 ± 0.07	0.37 ± 0.02
5	90nm_coated_135nm_3		1.61 ± 0.09	0.38 ± 0.01
6	SOA_1		2.06 ± 0.13	1.04 ± 0.01
6	SOA_2		2.26 ± 0.22	1.05 ± 0.01

Figure S1. Mobility size distributions of selected model aerosols. In green, the size distributions of soot particles with GMD_{mob} of 90 - 135 nm belonging to series no. 1 (Main manuscript, Table 1) are shown. The size distributions of particles with GMD_{mob} of 30 - 50 nm (series no. 3, Main manuscript, Table 1) are plotted in blue. The symbol "c" in the label denotes coated particles and the number designates the GMD_{mob} of the particles.

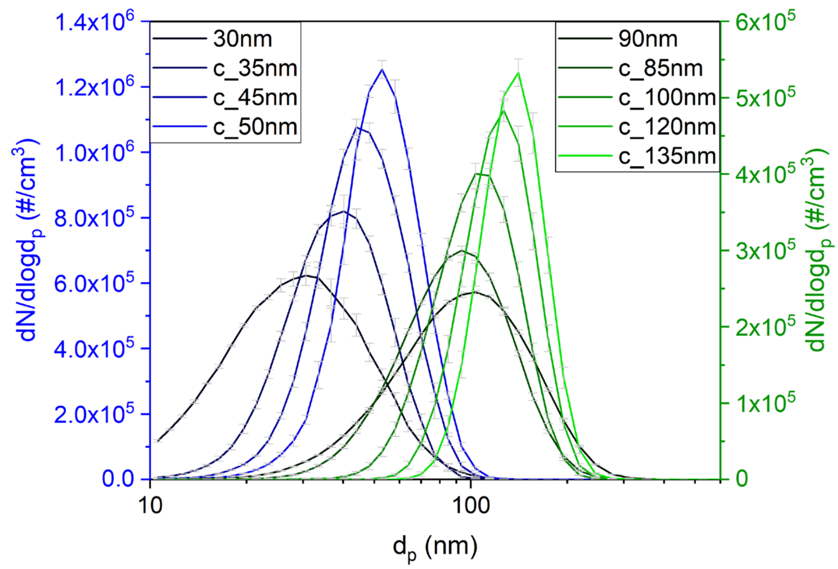

Figure S2: **Cryo-TEM images**. **(A)** uncoated soot particles with GMD_{mob} of 90 nm and soot particles coated with α-pinene SOM (series no. 1) having a nominal GMD_{mob} of **(B)** 85 nm, **(C)** 100 nm and **(D)** 120 nm. The Cryo-TEM images were used to obtain information on changes of the particle morphology upon coating with SOM.

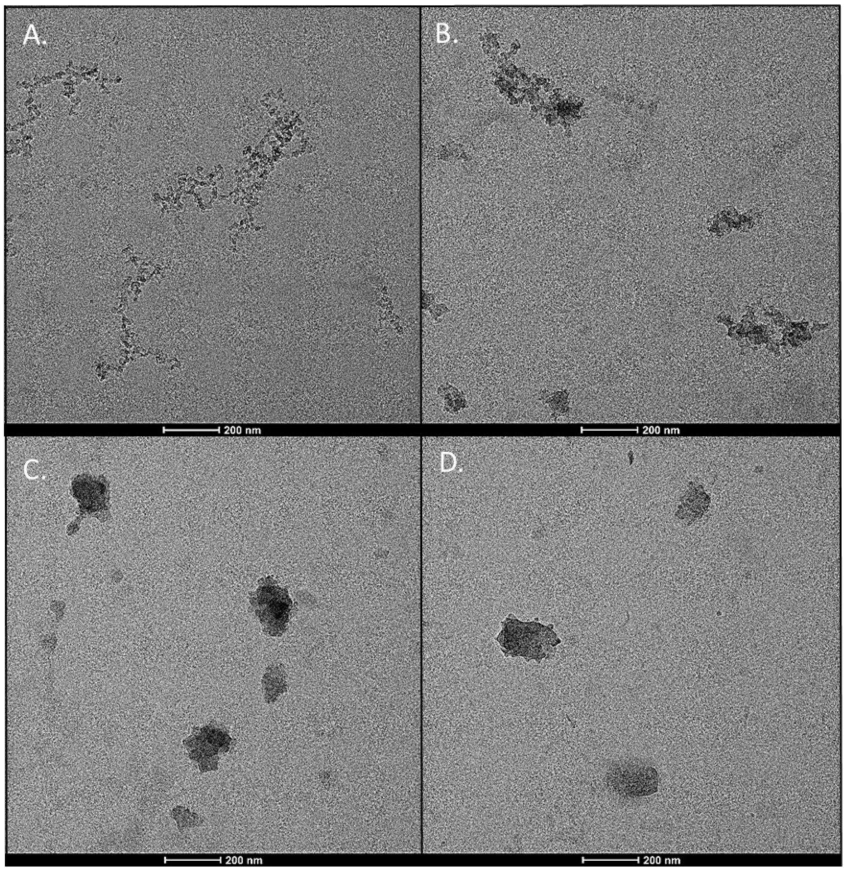

Table S2. Percentage of PAH mass to total soot mass (% w/w).

PAH	90 nm soot (% w/w)	30 nm soot (% w/w)
Phenantrene	0.030	0.328
Anthracene	0.000	0.004
Fluoranthene	0.002	0.066
Pyrene	0.002	0.089
Benz(a)anthracene	< DL*	< DL
Chrycene	0.000	0.000
Benzo(k,b,j)fluoranthene	0.000	0.000
Benzo(a)pyrene	< DL	< DL
Benzo (ghi)perylene	0.000	0.000
Indeno(1,2,3-cd)pyrene	< DL	0.000
Dibenz(a,h/a,c)anthracene	< DL	< DL
SUM	0.034	0.487

*DL stands for detection limit.

Aerosol mass spectrometry (AMS) was performed at the University of Manchester, UK. The material on the sampled filters was first extracted at the National Physical Laboratory, UK, using 45 mL of distilled water, sonicating at 40 °C for a period of 20 min. After sonication was complete, 5 mL of 100 mg/kg ammonium sulfate solution was added to the extract. The mass of both the distilled water and ammonium sulfate solution were recorded, and the mass fraction of the final extract calculated. The same procedure was also performed on two blank filters so that they could be used as AMS sample blanks. The extracts were then sent to the University of Manchester for analysis. Upon arrival at the analysis laboratory, each extract was filtered using disposable Millex GV 0.22 µm Durapore PVDF membranes. Each sample was analyzed in turn using a high-resolution AMS [8] operating under the default configuration with the vaporizer at 600 °C and using 70 eV electron ionization. Samples were atomized using plastic Colliston atomizer heads and the generated aerosols passed to the AMS via a silica gel diffusion drier. Each sample was measured for at least 300 s, with data was recorded every 30 s. A dwell time of 7.5 s was used. The two 'sample blanks' (see above) and a 'procedure blank' (deionized water) were analyzed in the same manner.

Data analysis was performed using the Squirrel 1.23l AMS data analysis software. Since ammonium sulfate was used as internal reference, ionization and collection efficiencies were not considered. Mass concentrations were calculated using the fragmentation table method of Allan et al. [9]. The default relative ionization efficiency values of sulfate and organics of 1.2 and 1.4, respectively, were used to calculate the organic concentration relative to sulfate. The background mass spectrum obtained from the sample blanks was subtracted from the mass spectrum of each sample The elemental and OM/OC ratios were calculated by the Pika 1.231 high-resolution analysis module, using weighted mass spectral fragment summation method described by Aiken et al. [10], incorporating the updated 'improved ambient' parameters as described by Canagaratna et al. [11].

Table S3. Elemental ratios (O/C, H/C) and ratio of water soluble organic mass (WSOM) to water soluble organic carbon (WSOC) for selected model aerosols.

Sample	VOC	WSOM/WSOC	O/C	H/C	$\overline{OS}$ **	Increase in $\overline{OS}$
90 nm*	-	1.66	0.37	1.99	-1.25	
c_85nm	α-pinene	1.89	0.55	1.77	-0.67	0.58
c_85nm		1.91	0.57	1.73	-0.59	0.66
c_100nm		1.82	0.50	1.72	-0.72	0.53
c_100nm		1.90	0.57	1.69	-0.55	0.70
c_120nm		1.78	0.48	1.71	-0.75	0.50
c_120nm		1.79	0.49	1.70	-0.73	0.52
SOA		1.85	0.53	1.69	-0.63	0.62
SOA		1.78	0.48	1.71	-0.75	0.50

* The data from the analysis of the second filter were discarded because of difficulties related to the extraction of particulate matter from the filter.

** The average carbon oxidation state $\overline{OS}$ was calculated as $\overline{OS} = 2 \cdot \mathrm{O/C} - \mathrm{H/C}$, where O/C and H/C are the molar oxygen-to-carbon and hydrogen-to-carbon ratios [12].

The average ozone concentration in the MSC was 60 ppm (120 mg m^{-3}) and the residence time of the particles in the MSC was 7.6 s. This corresponds to an ozone exposure of approximately 1.1×10^{16} molec cm^{-3} s. Based on the assumption that all reactions follow a first-order kinetic mechanism, the O_3 exposure can be expressed as equivalent atmospheric age in days by dividing the O_3 exposure by an average atmospheric O_3 concentration. Assuming an average atmospheric O_3 concentration of 35 ppb which equals a concentration of 8.2×10^{11} molec cm^{-3} at a temperature of 25 °C and a pressure of 965 mbar [13], the corresponding atmospheric age is estimated to be about 3.5 h.

Figure S3: Fraction plot of fCO_2^+ vs $f\ C_2H_3O^+$ for the samples described in Table 2. The dashed lines show the triangular space, suggested by [14], where ambient OOA components are typically found. The individual data points colors reflect the different experimental conditions for the samples described in Table S3.

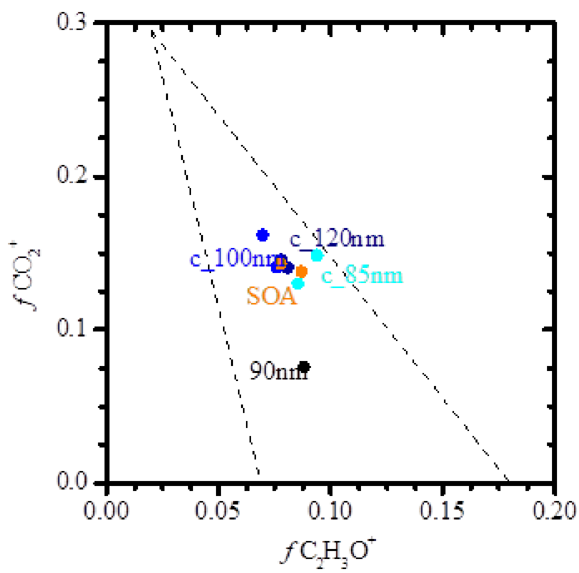

Figure S4: Normalized aerosol mass spectra for different experimental conditions. The different colors correspond to the average mass spectra of the experimental conditions described in Table S3. The reference spectrum was taken from the literature and corresponds to a dark ozonolysis experiment [15].

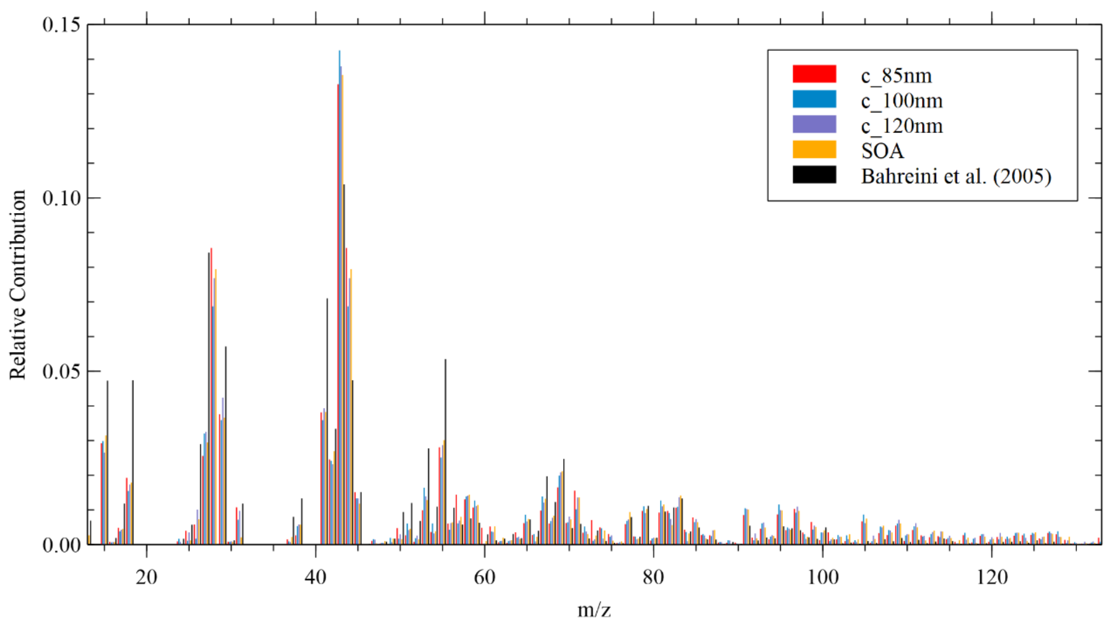

Table S4. Angle between normalized spectra for different experimental conditions. The angle describes their degree of similarity; SOM: Secondary organic matter [16]. The set points correspond to average mass spectra for the experimental conditions described in Table S3. The reference spectrum was taken from the literature and corresponds to a dark ozonolysis experiment [15].

Angles between Spectra (°)	c_85nm	c_100nm	c_120nm	SOA	Reference
c_85nm	0	9.7	7.0	6.6	38.9
c_100nm		0	6.3	6.9	35.7
c_120nm			0	4.7	35.7
SOA				0	36.8
Reference					0

Figure S5: Percentage of LDH release as a function of the deposited particle mass per cell culture area for series nos. 2 and 4 (mesitylene as SOM precursor). I.C.: incubator control.

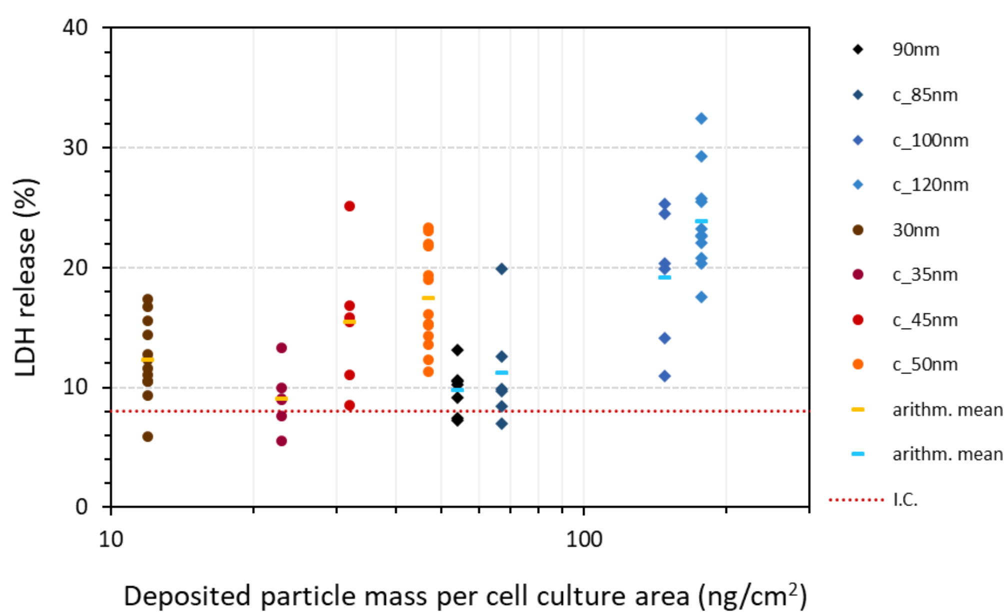

Table S5. Statistical significance and adjusted *p*-values. Tukey's multiple comparisons test

α-pinene: 30 nm series	**Statistical significance**	**Adjusted *p*-value**
c_30nm vs. c_35nm	ns	0.7583
c_30nm vs. c_45nm	*	0.0223
c_30nm vs. c_50nm	***	0.0001
c_35nm vs. c_45nm	ns	0.1587
c_35nm vs. c_50nm	***	0.0005
c_45nm vs. c_50nm	ns	0.0631
α-pinene: 90 nm series	**Statistical significance**	**Adjusted *p*-value**
c_90nm vs. c_85nm	ns	0.2249
c_90nm vs. c_100nm	ns	0.8937
c_90nm vs. c_120nm	**	0.0088
c_90nm vs. c_135nm	ns	0.4601
c_85nm vs. c_100nm	*	0.0381
c_85nm vs. c_120nm	***	0.0001
c_85nm vs. c_135nm	**	0.0079
c_100nm vs. c_120nm	ns	0.0671
c_100nm vs. c_135nm	ns	0.9193
c_120nm vs. c_135nm	ns	0.3709
Mesitylene: 30 nm series	**Statistical significance**	**Adjusted *p*-value**
c_30nm vs. c_35nm	ns	0.3759
c_30nm vs. c_45nm	ns	0.4059
c_30nm vs. c_50nm	*	0.0159
c_35nm vs. c_45nm	*	0.0424
c_35nm vs. c_50nm	***	0.0009
c_45nm vs. c_50nm	ns	0.7576
Mesitylene: 90 nm series	**Statistical significance**	**Adjusted *p*-value**
90nm vs. c_85nm	ns	0.9234
90nm vs. c_100nm	**	0.0026
90nm vs. c_120nm	***	0.0001
c_85nm vs. c_100nm	*	0.0162
c_85nm vs. c_120nm	***	0.0001
c_100nm vs. c_120nm	ns	0.1599

Figure S6. Proteome analysis of cells exposed to 30 nm and 90 nm soot particles. (A) and (C): Exposure to 30 nm and 90 nm soot particles coated with oxidation products of α-pinene. **(B) and (D):** Exposure to 30 nm and 90 nm soot particles coated with oxidation products of mesitylene. Fold changes of cytokines and chemokines relative to unexposed cells (Inc. Ctrl: incubator control).

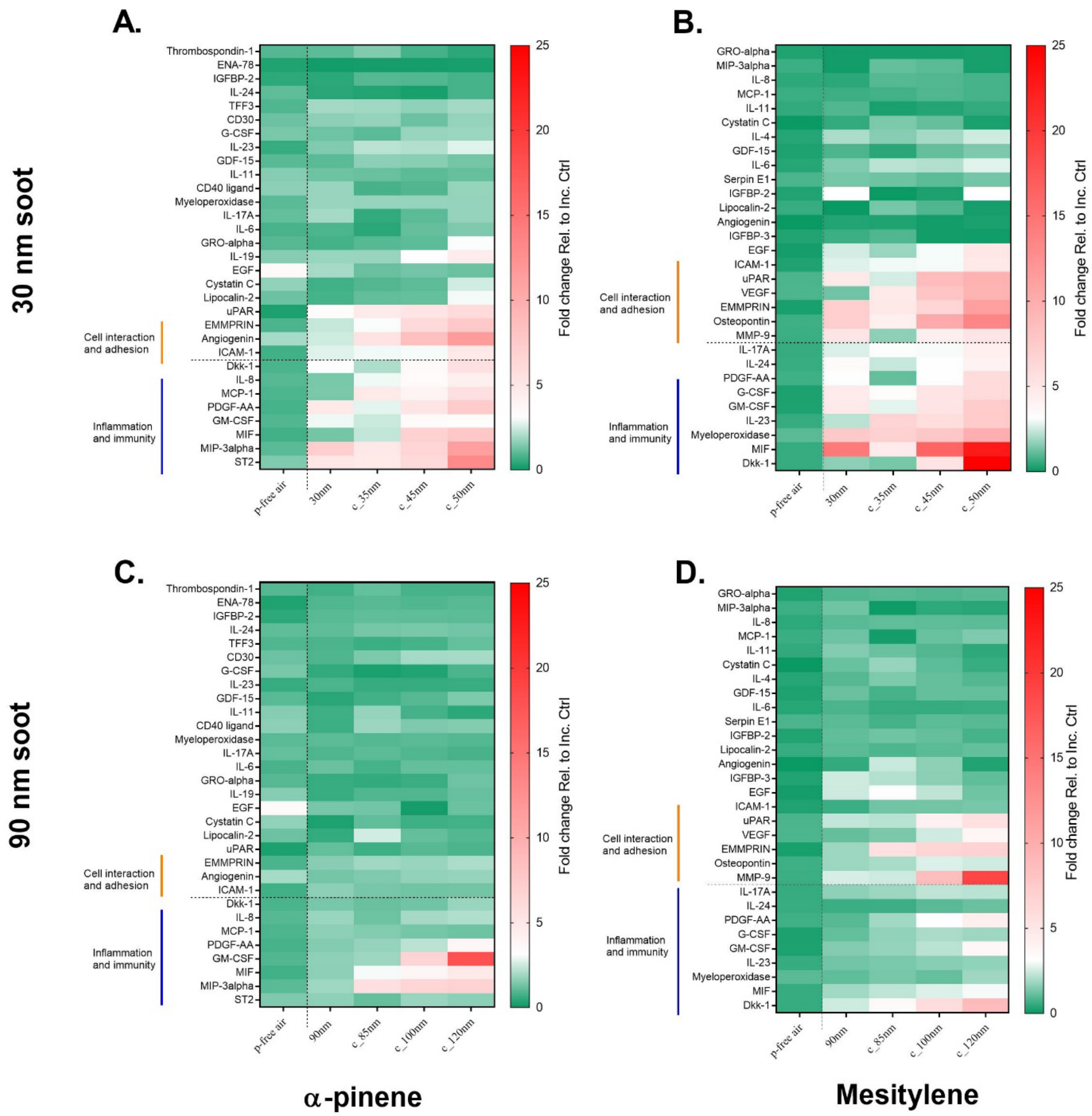

Figure S7: **Proteome analysis of cells exposed to coated α-pinene particles.** Fold changes of cyto- and chemokines expression are relative to unexposed cells (Inc. Ctrl: incubator control). Abbreviations: uPAR: Urokinase-type plasminogen activator receptor; EMMPRIN: Extracellular matrix metalloproteinase inducer; ICAM-1: Intercellular adhesion molecule 1; Dkk-1: Dickkopf WNT signaling pathway inhibitor 1; IL-8: Interleukin-8; MCP-1: Monocyte chemoattractant protein-1; PDGF-AA: Platelet-derived growth factor-AA; GM-CSF: Granulocyte-macrophage colony-stimulating factor; MIF: Macrophage migration inhibitory factor; MIP-3alpha: Macrophage inflammatory protein 3 alpha; ST2: Interleukin 1 receptor-like 1; SOM: Secondary organic matter.

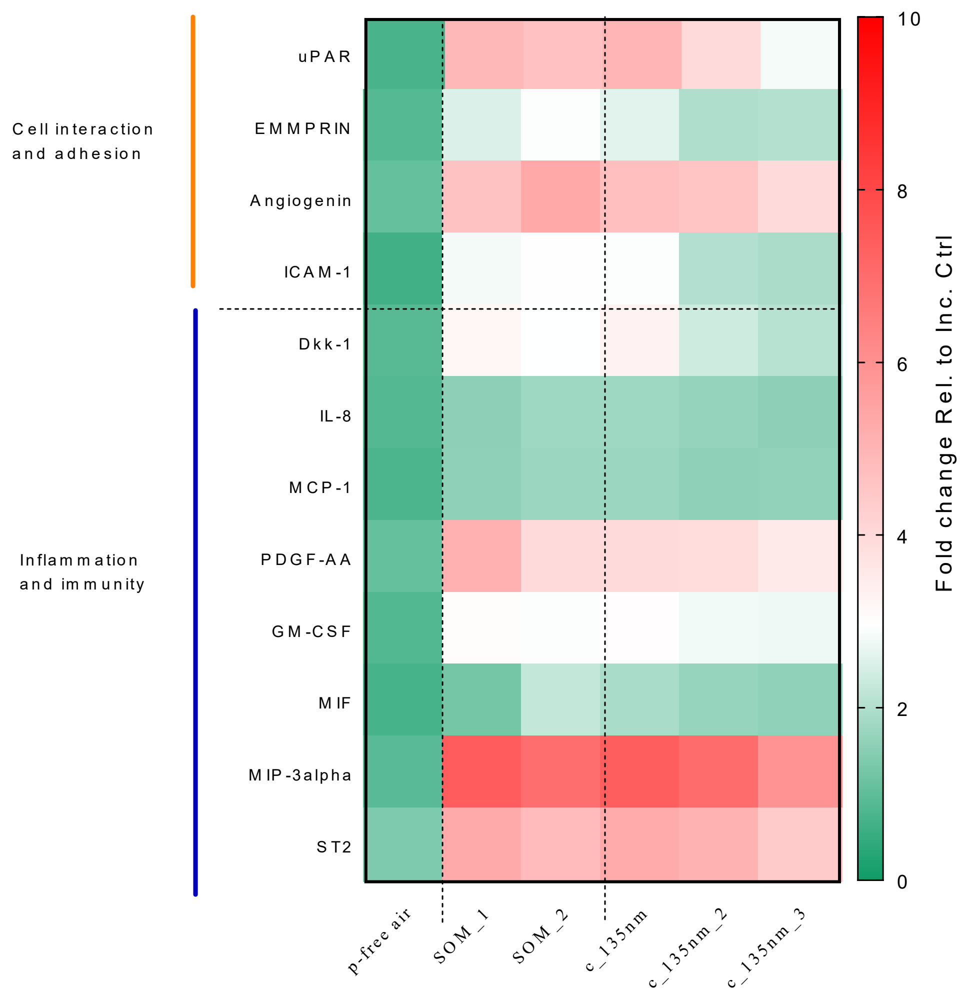

REFERENCES

(1) Drinovec, L.; Močnik, G.; Zotter, P.; Prévôt, A. S. H. H.; Ruckstuhl, C.; Coz, E.; Rupakheti, M.; Sciare, J.; Müller, T.; Wiedensohler, A.; et al. The "Dual-Spot" Aethalometer: An Improved Measurement of Aerosol Black Carbon with Real-Time Loading Compensation. *Atmos. Meas. Tech.* **2015**, *8* (5), 1965–1979.

(2) Arnott, W. P.; Moosmüller, H.; Walker, J. W. Nitrogen Dioxide and Kerosene-Flame Soot Calibration of Photoacoustic Instruments for Measurement of Light Absorption by Aerosols. *Rev. Sci. Instrum.* **2000**, *71* (12), 4545–4552.

(3) Nakayama, T.; Suzuki, H.; Kagamitani, S.; Ikeda, Y. Characterization of a Three Wavelength Photoacoustic Soot Spectrometer (PASS-3) and a Photoacoustic Extinctiometer (PAX). *J. Meteorol. Soc. Japan* **2015**, *93* (2), 285–308.

(4) ISO 12884. ISO 12884:2000 Ambient Air — Determination of Total (Gas and Particle-Phase) Polycyclic Aromatic Hydrocarbons — Collection on Sorbent-Backed Filters with Gas Chromatographic/Mass Spectrometric Analyses. **2000**.

(5) ISO 15549. ISO 15549:2019 Non-Destructive Testing — Eddy Current Testing — General Principles. **2019**.

(6) Hellén, H.; Kangas, L.; Kousa, A.; Vestenius, M.; Teinilä, K.; Karppinen, A.; Kukkonen, J.; Niemi, J. V. Evaluation of the Impact of Wood Combustion on Benzo[a] Pyrene (BaP) Concentrations; Ambient Measurements and Dispersion Modeling in Helsinki, Finland. *Atmos. Chem. Phys.* **2017**, *17*, 3475–3487.

(7) Jeannet, N.; Fierz, M.; Kalberer, M.; Burtscher, H.; Geiser, M. Nano Aerosol Chamber for In-Vitro Toxicity (NACIVT) Studies. *Nanotoxicology* **2015**, *9* (1), 34–42.

(8) DeCarlo, P. F.; Kimmel, J. R.; Trimborn, A.; Northway, M. J.; Jayne, J. T.; Aiken, A. C.; Gonin, M.; Fuhrer, K.; Horvath, T.; Docherty, K. S.; et al. Field-Deployable, High-Resolution, Time-of-Flight Aerosol Mass Spectrometer. *Anal. Chem.* **2006**, *78* (8), 281–8289.

(9) Allan, J. D.; Coe, H.; Bower, K. N.; Alfarra, M. R.; Delia, A. E.; Jimenez, J. L.; Middlebrook, A. M. Drewnick, F.; Onasch, T. B. Canagaratna, M. R.; Jayne, J. T.; Worsnop, D. R. A Generalised Method for the Extraction of Chemically Resolved Mass Spectra from Aerodyne Aerosol Mass Spectrometer Data. *J. Aerosol Sci.* **2004**, *35*, 909-922,.

(10) Aiken, A. C.; DeCarlo, P. F.; Kroll, J. H.; Worsnop, D. R.; Huffman, J. A.; Docherty, K. S.; Ulbrich, I. M.; Mohr, C.; Kimmel, J. R.; Sueper, D.; et al. O/C and OM/OC Ratios of Primary , Secondary, and Ambient Organic Aerosols with High-Resolution Time-of-Flight Aerosol Mass Spectrometry. *Environ. Sci.Technol.* **2008**, *42* (12), 4478–4485.

(11) Canagaratna, M. R.; Jimenez, J. L.; Kroll, J. H.; Chen, Q.; Kessler, S. H.; Massoli, P.; Hildebrandt Ruiz, L.; Fortner, E.; Williams, L. R.; Wilson, K. R.; et al. Elemental Ratio Measurements of Organic Compounds Using Aerosol Mass Spectrometry: Characterization, Improved Calibration, and Implications. *Atmos. Chem. Phys.* **2015**, *15*, 253–272.

(12) Kroll, J. H.; Lim, C. Y.; Kessler, S. H.; Wilson, K. R. Heterogeneous Oxidation of Atmospheric Organic Aerosol: Kinetics of Changes to the Amount and Oxidation State of Particle-Phase Organic Carbon. *J. Phys. Chem. A* **2015**, *119* (44), 10767–10783.

(13) Friebel, F.; Mensah, A. A. Ozone Concentration versus Temperature: Atmospheric Aging of Soot Particles. *Langmuir* **2019**, *35* (45), 14437–14450.

(14) Ng, N. L.; Canagaratna, M. R.; Zhang, Q.; Jimenez, J. L.; Tian, J.; Ulbrich, I. M.; Kroll, J. H.; Docherty, K. S.; Chhabra, P. S.; Bahreini, R.; et al. Organic Aerosol Components Observed in Northern Hemispheric Datasets from Aerosol Mass Spectrometry. *Atmos. Chem. Phys.* **2010**, *10* (10), 4625–4641.

(15) Bahreini, R.; Keywood, M. D.; Ng, N. L.; Varutbangkul, V.; Gao, S.; Flagan, R. C.; Seinfeld, J. H.; Worsnop, D. R.; Jimenez, J. L. Measurements of Secondary Organic Aerosol from Oxidation of Cycloalkenes, Terpenes, and m-Xylene Using an Aerodyne Aerosol Mass Spectrometer. *Environ. Sci. Technol.* **2005**, *39* (15), 5674–5688.

(16) Kostenidou, E.; Lee, B. H.; Engelhart, G. J.; Pierce, J. R.; Pandis, S. N. Mass Spectra Deconvolution of Low, Medium, and High Volatility Biogenic Secondary Organic Aerosol. *Environ. Sci. Technol.* **2009**, *43* (13), 4884–4889.